Gigahertz characterization of a single carbon nanotube

L. Nougaret, Gilles Dambrine, Sylvie Lepilliet, H. Happy, N. Chimot, Vincent Derycke, J.P. Bourgoin

Applied Physics Letters

Gigahertz characterization of a single carbon nanotube

Cite as: Appl. Phys. Lett. **96**, 042109 (2010); https://doi.org/10.1063/1.3284513
Submitted: 08 July 2009 • Accepted: 25 November 2009 • Published Online: 28 January 2010

L. Nougaret, G. Dambrine, S. Lepilliet, et al.

Gigahertz characterization of a single carbon nanotube

L. Nougaret,[1] G. Dambrine,[1] S. Lepilliet,[1] H. Happy,[1,a)] N. Chimot,[2] V. Derycke,[2] and J.-P. Bourgoin[2]
[1]*Institut d'Electronique, de Microélectronique, et de Nanotechnologie, UMR-CNRS 8520, BP 60069, Avenue Poincaré, 59652 Villeneuve d'Ascq Cedex, France*
[2]*Laboratoire d'Electronique Moléculaire, Service de Physique de l'Etat Condensé (CNRS URA 2464), CEA, IRAMIS, 91191 Gif sur Yvette, France*

(Received 8 July 2009; accepted 25 November 2009; published online 28 January 2010)

Carbon nanotubes are intrinsically high impedance objects. The high frequency (HF) characterization of these nano-objects is crucial for applications such as interconnects in future integrated circuits, but still represents a daunting challenge. This letter presents HF characterization of an individual metallic single walled carbon nanotube up to 7 GHz. The equivalent circuit values are directly extracted from these HF measurements without numerical procedure, thus proving that the intrinsic transport parameters of a single carbon nanotube can be determined up to gigahertz frequencies. © *2010 American Institute of Physics*. [doi:10.1063/1.3284513]

Carbon nanotubes (CNTs) are attractive candidates for high frequency (HF) electronics because of their unique electrical properties.[1,2] In particular, they could serve as both efficient interconnects and small size field effect transistors. Recently, CNT-based field effect transistor (CNTFET) with intrinsic cutoff frequency as high as 80 GHz,[3,4] where demonstrated, bringing support to the theoretical predictions.[5–8] CNT interconnects operating in the gigahertz (GHz) range were also realized.[9]

Despite these encouraging results and the constant progresses made toward a CNT technology,[10] the issue of measuring the GHz transport properties of a single, or a very few, nano-object(s), is still blocking the development of HF circuits based on nano-objects.[2] Indeed, CNTs have an intrinsic high impedance (HI), well above the impedances (50 Ω) at which conventional electronic and measurement systems can be adapted at GHz frequencies. Due to the impedance mismatch, the measurement accuracy is not sufficient to extract the intrinsic parameters of these nano-objects. Several works were recently published on this subject.[1,2,11–14]

In this work, we have developed a HI integrated set-up system[15] to measure, in one-port, the HF properties of nanodevices. The nanodevice is integrated in a measurement system illustrated in Fig. 1(a), based on a Wheatstone bridge structure. This structure acts as a directive coupler that separates the incident and reflective waves. Moreover, the resistances of the bridge (in the range of 700 Ω to 3.5 kΩ) contribute to reduce the impedance mismatch between the vectorial network analyzer (VNA) and the CNT,[5] and thus minimize the measurement error.

The Wheatstone bridge structure, shown in Fig. 1(a), is an integrated device, only few hundred micrometers in size. The structure is fabricated on a high resistivity Si substrate (resistivity > 8000 Ω cm) covered with SiO_2 film deposited by low pressure chemical vapor deposition (LPCVD). It is composed of three identical resistances, and the nanodevice under characterization [here single walled carbon nanotube (SWNT)—1 μm length between contact pads] is inserted in the fourth branch. To this end, fabrication techniques similar to those of CNTFET are used [Fig. 1(b)]. The complete description of device fabrication is made in Ref. 17.

Figure 1(a) shows also a synoptic of the measurement set-up. The Wheatstone bridge is connected to the port 1 of the VNA using ®Infinity GSG (Ground Signal Ground) probes from Cascade Microtech. As shown in Fig. 1(a), a HI passive probe (Cascade Microtech® FPM x100, 5 kΩ–50 Ω) is connected to the port 2 of the VNA via a broadband low noise amplifier (20 dB gain). This amplifier compensates the signal attenuation across HI probe. The experimental Wheatstone technique is based on a differential measurement to determine the reflection coefficient of the device under test (D_{DUT})—here SWNT-using the following relation: $D_{DUT} = S_{p1\_DUT} - S_{p2\_DUT}$. The HI probe contacts successively the pads p1 and p2, which are specified in Fig. 1(a). The VNA is noncalibrated. The calibration is realized

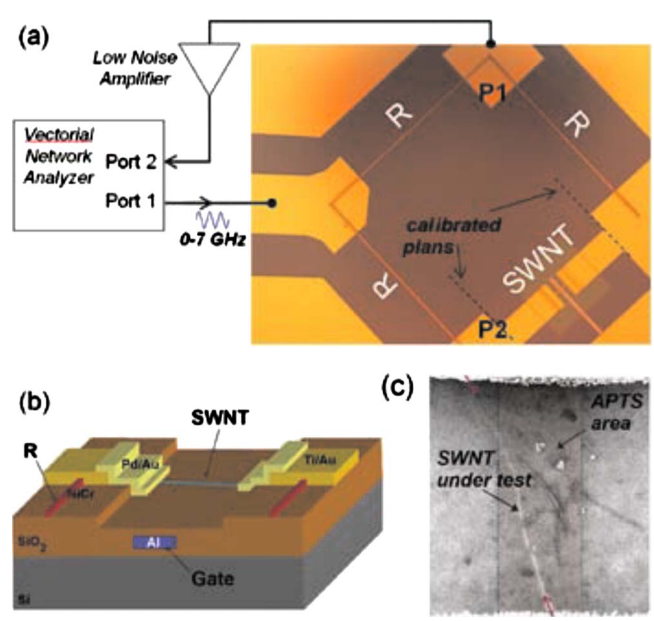

FIG. 1. (Color online) Measurement structure: (a) top view of Wheatstone bridge and synoptic of the measurement set-up; (b) Cross section of the SWNT structure under test; (c) SEM picture of one SWNT onto APTS zone and connected by Pd/Au at its extremities.

a)Author to whom correspondence should be addressed. Electronic mail: henri.happy@iemn.univ-lille1.fr.

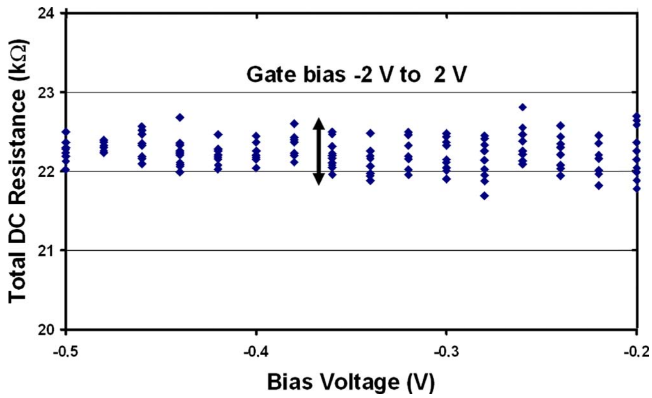

FIG. 2. (Color online) Measurement of total dc resistance vs bias voltage, as a function of gate voltage.

with short (CC), open (CO), and equilibrated bridge (Z_c) integrated on the same wafer as the DUT ones. Calibration procedure and validation is described in Ref. 17.

Let us now show the interest of this system in the concrete case of individual metallic SWNT measurements. To increase measurement bandwidth, the Wheatstone bridge resistance of 1 kΩ is used. As a first step, the dc value of a SWNT resistance is measured using the Wheatstone bridge as an Ohm-meter. I(V) measurements are shown in Fig. 2 after removing the influence of the bridge's resistances. The measured dc resistance of this SWNT is close to 22 kΩ. By applying dc voltage on the gate (±2 V), we noticed no significant variation of the current and deduced that this individual SWNT is metallic.

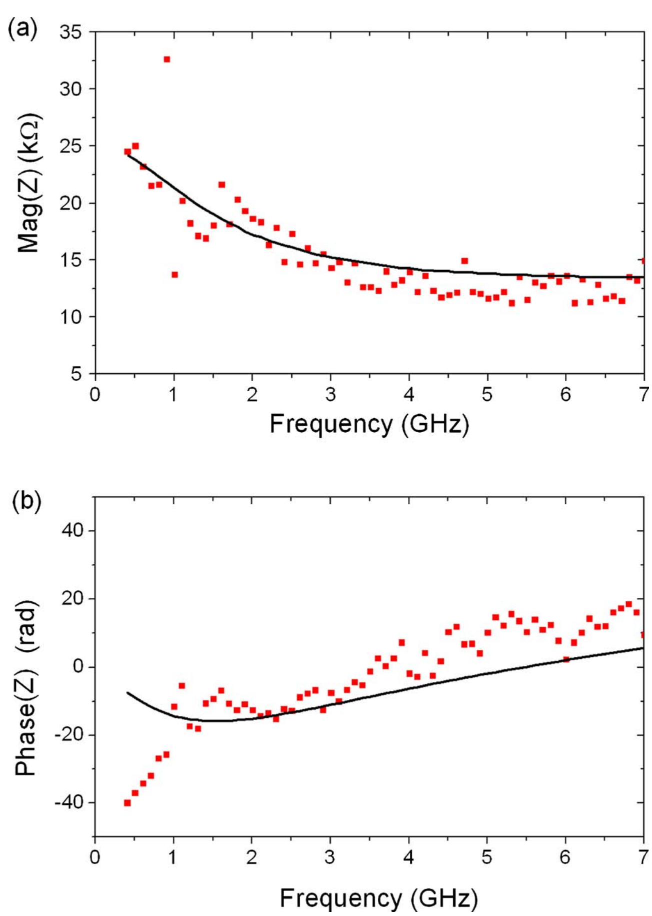

FIG. 3. (Color online) Impedance response of SWNT vs frequency in term of magnitude (a) and phase (b). Measured impedance (points) and calculated impedance derivate from equivalent circuit (line).

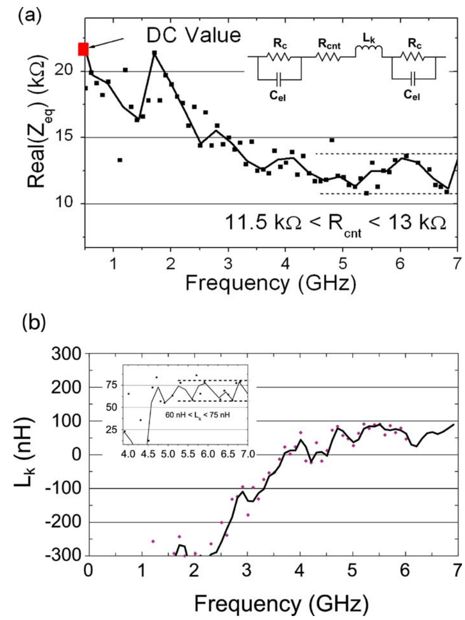

FIG. 4. (Color online) Extraction of small signal equivalent circuit of metallic SWNT derived from measurement at high frequency: (a) Illustration of equivalent circuit and extraction of resistance (R_{cnt}), (b) extraction of inductance: (L_k) is obtained at HF as illustrated in the inset.

The frequency response up to 7 GHz, obtained with this individual metallic SWNT is presented in Figs. 3(a) and 3(d). Such frequency response corresponds approximately to one of the equivalent circuits shown in inset of Fig. 4(a). This circuit is described by the following expression:

$$Z_{eq} = \frac{2}{Y_c} + Z_{CNT}, \quad \text{where} \quad Z_{CNT} = R_{CNT} + jL_k\omega$$

$$\text{and} \quad Y_c = \frac{1}{R_c} + jC_{el}\omega,$$

Z_{CNT} is the SWNT impedance and Y_c is the admittance of one contact. We assume that this dipole is symmetrical.

The parameters of this equivalent circuit are directly deduced from measurements, with some hypothesis. Figure 4(a) represents the real part of the connected metallic SWNT impedance, under 0 V gate bias conditions. We can observe two frequency areas; up to 3 GHz, the impedance decreases from 25 to 15 kΩ and remains almost constant for higher frequencies. Then, in the higher frequency range, we extract directly, from the real part of the measured impedance the value of R_{cnt} between 11.5 and 13 kΩ. Figure 4(b) plots the imaginary part of $(Z_{meas})/\omega$. From this figure, it appears that for frequency greater than 4.5 GHz, the curve is frequency independent, that leads a value of an inductance L_k between 60 and 75 nH [Fig. 4(b)].

By removing this "R_{CNT} L_k" series dipole from measurements, we can extract in the lower frequency range the values of the "R_c C_{el}" parallel dipole named Y_{cmeas}. Figures 5(a) and 5(b) plot R_c and C_{el} extracted from measurement of $2/[\text{real}(Y_{cmeas})]$ and $2.\text{imag}(Y_{cmeas})/\omega$, respectively. The equivalent contact resistance R_c extracted is between 4 and 6 kΩ while the equivalent contact capacitance C_{el} is between 10 and 25 fF. We note that the total resistance (R_{CNT}

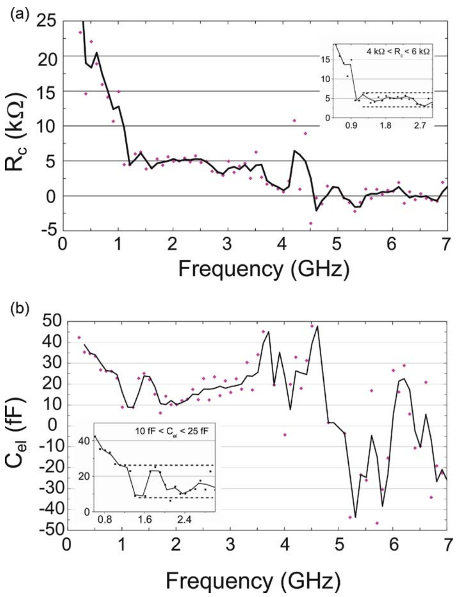

FIG. 5. (Color online) Extraction of small signal equivalent circuit of SWNT contact parameters at low frequency: (a) Extraction of contact resistance (R_c), (b) extraction of capacitance (C_{el}). The insets illustrated area of extraction. Beyond the cut-off frequency, extractions are not significant.

$+2R_c$) is in quite good agreement with the resistance of the contacted SWNT measured in dc characteristic (Fig. 2).

We report in Figs. 3(a) and 3(b) the comparison of the measured and calculated impedance (magnitude and phase) of the contacted SWNT up to 7 GHz. The respective values of equivalent circuit used [illustrated in Fig. 4(a) inset] are: $R_{CNT}=12.25$ kΩ, $L_k=67$ nH, $R_c=5$ kΩ, and $C_{el}=17.5$ fF. These values are chosen as the mean values of extracted parameters. The experimental results call for the following comments.

The value of $R_{CNT}\sim 12.5$ kΩ deduced from this measurement is in agreement with dc values obtained in previous works.[13,15] The inductance $L_k\sim 70$ nH is comparable to those obtained in Ref. 1, but is almost three to four times higher than the theoretical value[2,6] (16 nH/μm).

The value of contact resistance corresponds to values depicted in literature.[1,2,6,16] In addition, the electrostatic capacitance; C_{el} ($\sim$17 fF) is two orders of magnitude higher than theoretical value and one order of magnitude higher than those obtained in Ref. 1. We assume the divergence with the theoretical values can be associated to a diffusive behavior. Theoretical model[4] assumes ballistic transport. In addition, we think C_{el} value is screened by parasitic capacitances. Indeed the measurement calibration plane is far from the SWNT plane.

In this letter, a HI characterization that allows measurement of the frequency response up to 7 GHz has been presented. Based on integrated HI Wheatstone structures, we have accurately measured the reflection coefficient of an individual CNT. From these measurements, an equivalent circuit of a single metallic SWNT is directly deduced. The values of the parameters of this equivalent circuit are comparable to other published results, and can still be improved by reducing parasitics introduced by the reference plane of calibration. Such new set-up can be extended to the characterization of various nano-objects with HI.

[1] J. J. Plombon, K. P. O'Brien, F. Gstrien, and V. M. Dubin, Appl. Phys. Lett. **90**, 063106 (2007).
[2] C. Rutherglen, D. Jain, and P. J. Burke, Appl. Phys. Lett. **93**, 083119 (2008).
[3] A. Le Louarn, F. Kapche, J.-M. Bethoux, H. Happy, G. Dambrine, V. Derycke, P. Chenevier, N. Izard, F. Goffman, and J.-P. Bourgoin, Appl. Phys. Lett. **90**, 233108 (2007).
[4] L. Nougaret, H. Happy, G. Dambrine, V. Derycke, J. -P. Bourgoin, A. A. Green, and M. C. Hersam, Appl. Phys. Lett. **94**, 243505 (2009).
[5] P. J. Burke, Z. Yu, and C. Rutherglen, in *Nanowires and Nanotubes*, edited by P. J. Burke (World Scientific, Singapore, 2007); M. P. Anantram and F. Leonard, Rep. Prog. Phys. **69**, 507 (2006).
[6] P. J. Burke, IEEE Trans. Nanotechnol. **2**, 55 (2003).
[7] D. V. Singh, K. A. Jenkins, J. Appenzeller, D. Neumayer, A. Grill, and H. S. P. Wong, IEEE Trans. Nanotechnol. **3**, 383 (2004).
[8] H. Cazin d'Honincthun, A. Bournel, S. Galdin, P. Dollfus, and J. P. Bourgoin, C. R. Phys. **9**, 67 (2008).
[9] G. F. Close, S. Yasuda, B. Paul, S. Fujita, and H.-S. P. Wong, Nano Lett. **8**, 706 (2008).
[10] Q. Cao and J. A. Rogers, Nano Res. **1**, 259 (2008).
[11] A. Tselev, M. Woodson, C. Qian, and J. Liu, Nano Lett. **8**, 152 (2008).
[12] P. Avouris, J. Appenzeller, R. Martel, and S. J. Wind, Proc. IEEE **91**, 11 (2003).
[13] P. J. Burke, Solid-State Electron. **48**, 1981 (2004).
[14] D. L. Pulfrey, D. L. John, and L. C. Castro, Proceedings of the 13th International Workshop on Physics of Semiconductor Devices (Dehli, 2005), p. 7–13.
[15] L. Nougaret, G. Dambrine, H. Happy, V. Derycke, and J.-P. Bourgoin, Patent deposed INPI conservatoire No. 08 07450 (24 December 2008).
[16] J. Kong, E. Yenilmez, T. W. Tombler, W. Kim, and H. Dai, Phys. Rev. Lett. **87**, 106801 (2001).
[17] See supplementary material at http://dx.doi.org/10.1063/1.3284513 for complete description of device fabrication, calibration techniques, deembedding procedure, and validation of method on high impedance resistance.